# Numerical Techniques to Model Fractional-Order Nonlinear Viscoelasticity in Soft Elastomers

## Presenter: Paul Miles

Authors: Paul R. Miles[a], Graham T. Pash[a,b], William S. Oates[c], Ralph C. Smith[a]

[a]Department of Mathematics, North Carolina State University
[b]Department of Mechanical Engineering, North Carolina State University
[c]Department of Mechanical Engineering, Florida A&M University and Florida State University

# Motivation

- Applications:
  - Robotics
  - Flow control
  - Energy harvesting
  - Optical switches

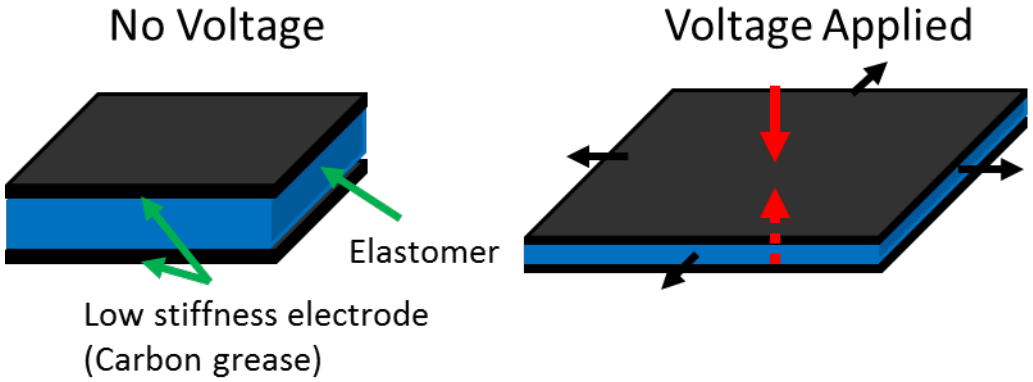


Figure: Out of plane expansion of elastomer as a result of transverse field.

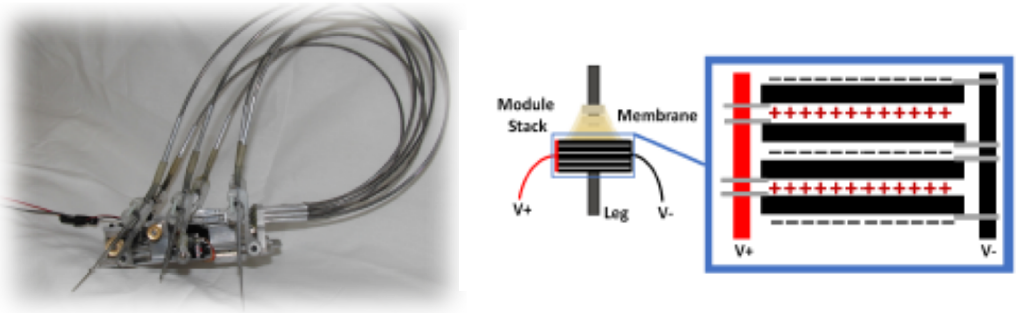


Figure: iSprawl robotic platform[1]. Membrane actuators control leg stiffness allowing for dynamic adaptation to different terrains.

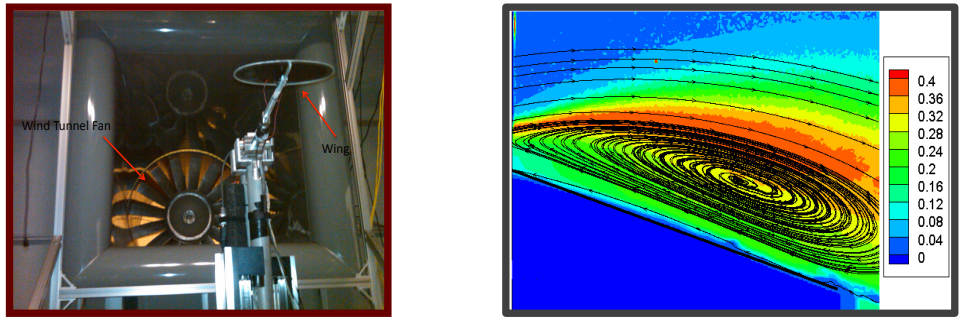


Figure: Wind tunnel experiments with deformable dielectric membrane[2]. By adjusting the membrane stiffness, the wing profile subsequently changed its shape and altered the flow characteristics.

1. Newton, J., "Design and Characterization of a Dielectric Elastomer Based Variable Stiffness Mechanism for Implementation onto a Dynamic Running Robot," (2014), Figure 2.11 and Figure 4.5.
2. Hays, et al. "Aerodynamic Control of Micro Air Vehicle Wings Using Electroactive Membranes," J. Mater. Syst. Struct., v. 24(7), pp. 862-878, 2013.

# Experimental Observations

- Hysteresis
- Stress response decays
- Recovery
- Steady state

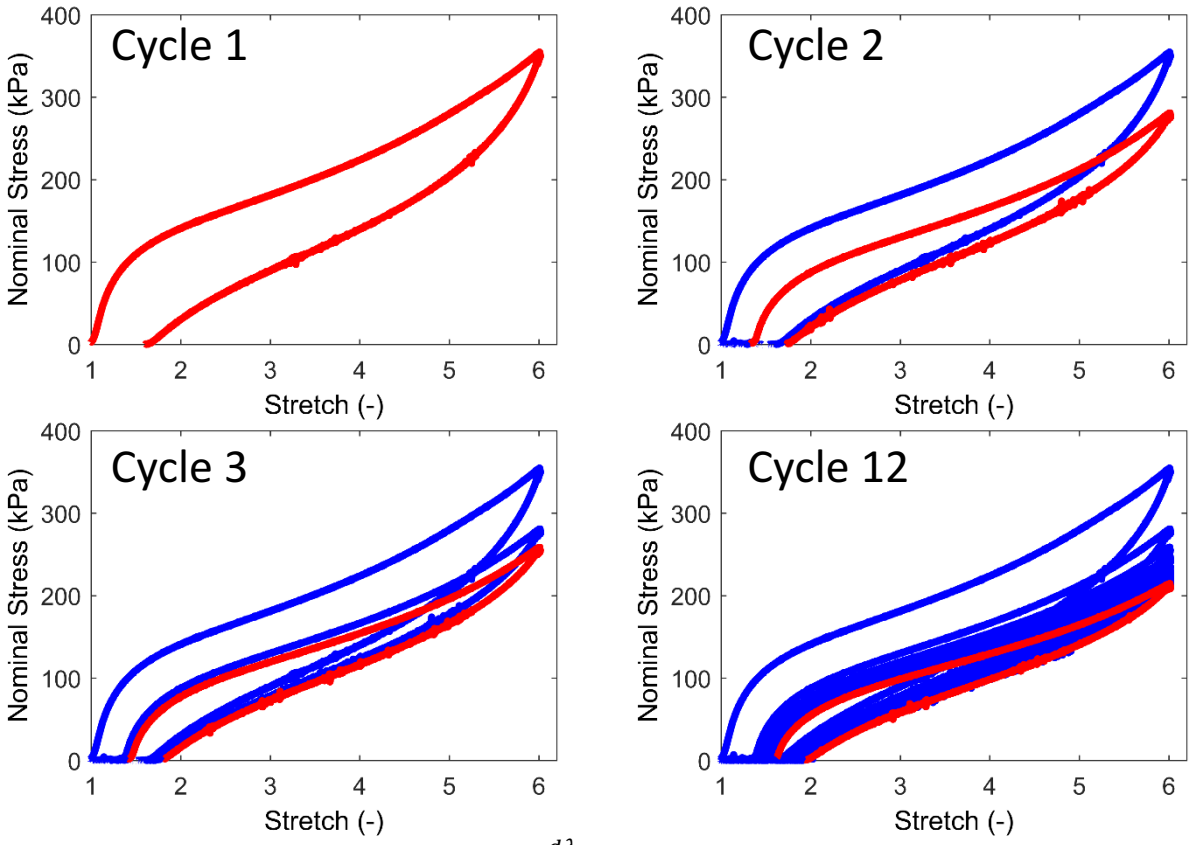


Figure: Cyclic loading of VHB 4910 at $\frac{d\lambda}{dt} = 0.67\ Hz$. Steady state hysteresis observed by the 12$^{th}$ cycle.

# Experimental Observations

- Steady state hysteresis
- Rate-dependence
- Uncertainty
  - Measurement
  - Specimen variability
- Difficult to model

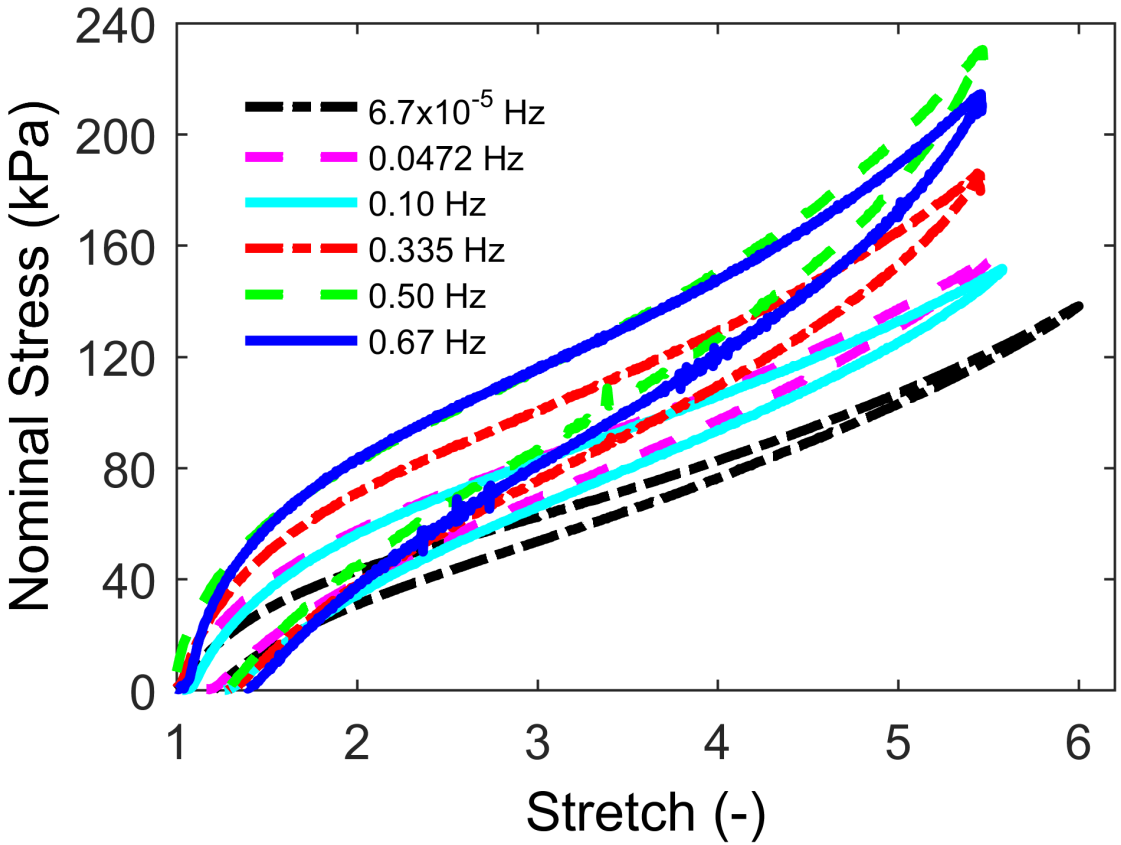


Figure: Steady state hysteresis loops from all stretch rates tested.

# Theory:

- Total Energy Density: $\psi = \psi_\infty(F_{iK}, \Theta) + \Upsilon(F_{iK}, \Theta, \xi_{iK})$
  - $F_{iK}$ - deformation gradient
  - $\Theta$ - temperature
  - $\xi_{iK}$ - set of non-conserved internal strains
- Conserved, hyperelastic energy function[1]

$$\psi_\infty = \frac{1}{6} G_c I_1 - G_c \lambda_{max}^2 \log(3\lambda_{max}^2 - I_1) + G_e \sum_j (\lambda_j + \frac{1}{\lambda_j})$$

- Non-conserved nonlinear energy function:

$$\Upsilon = \frac{1}{2} \gamma \xi_{iK} \xi_{iK} - \beta_\infty \frac{\partial \psi_\infty}{\partial F_{iK}} \xi_{iK} + \beta_\infty \psi_\infty$$

- Model Parameters
  - $G_c$ - Crosslink modulus
  - $G_e$ - Entanglement modulus
  - $\lambda_{max}$ - Maximum extension of affine tube
  - $\gamma$ - Proportional to viscosity of polymer network

1. Davidson, Jacob D., and N. C. Goulbourne. "A nonaffine network model for elastomers undergoing finite deformations." Journal of the Mechanics and Physics of Solids 61.8 (2013): 1784-1797.

# Theory:

- Nominal Stress

$$s_{iK} = \frac{\partial \hat{\psi}}{\partial F_{iK}} = \frac{\partial \psi_\infty}{\partial F_{iK}} - pJH_{iK} + \frac{\partial \Upsilon}{\partial F_{iK}}$$

- Viscoelastic constitutive law:[1,2]

$$Q_{iK}^{v} = \eta \left( \frac{d\xi_{iK}}{dt} \right) \rightarrow Q_{iK} = \eta D_t^{\alpha} s_{iK}^{\infty}$$

- Viscoelastic Stress

$$\frac{\partial \Upsilon}{\partial F_{iK}} = \beta_\infty \left( s_{iK}^{\infty} - \frac{\partial s_{iK}^{\infty}}{\partial F_{iK}} \left( \frac{1}{\gamma} \left( \beta_\infty s_{iK}^{\infty} - \eta D_t^{\alpha} s_{iK}^{\infty} \right) \right) \right)$$

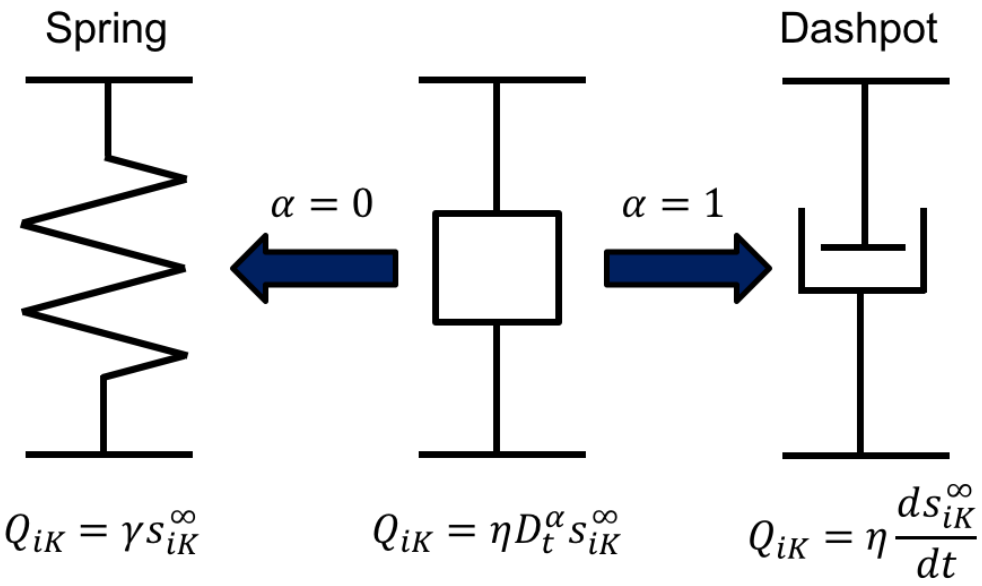


Figure: Fractional order spring-dashpot system. As the fractional order approaches 0 the system behaves like a dashpot. Likewise, as the fractional order approaches 1 the system behaves like a spring.

$D_t^{\alpha} s_{iK}^{\infty}$ - Fractional derivative?


1. Miles, P., Hays, M., Smith, R., Oates, W., "Bayesian Uncertainty Analysis of Finite Deformation Viscoelasticity." *Mechanics of Materials*, 2015, Vol. 91, pp. 35-49.
2. Mashayekhi, S., Miles, P., Hussaini, M. Y., Oates, W., "Fractional Viscoelasticity in Fractal and Non-Fractal Media: Theory, Experimental Validation, and Uncertainty Analysis." *Journal of the Mechanics and Physics of Solids*, 2017, Vol. 111, pp. 134-156.

# Fractional Derivative

- Riemann-Liouville Definition:

$$D_t^{\alpha}[f(t)] = \frac{1}{\Gamma(n-\alpha)} \frac{d^n}{dt^n} \int_0^t \frac{f(s)}{(t-s)^{\alpha+1-n}} ds,$$

where $n = \lceil \alpha \rceil$.

- Consider regime where $\alpha \in [0,1) \rightarrow n = 1$.

$$D_t^{\alpha}[f(t)] = \frac{1}{\Gamma(1-\alpha)} \frac{d}{dt} \int_0^{t} \frac{f(s)}{(t-s)^{\alpha}} ds.$$

- Singularity at upper integration limit.

# Fractional Derivative: Numerical Approach

$$D_t^{\alpha}[f(t)] = \frac{1}{\Gamma(1-\alpha)}\frac{d}{dt}\int_0^t \frac{f(s)}{(t-s)^{\alpha}}\,ds.$$

- Grünwald-Letnikov (GL): Reference – Extended Precision

$$D_{GL}^{\alpha}[f(t)] = \lim_{h\to 0}\frac{1}{h^{\alpha}}\sum_{0\le m<\infty}(-1)^m\binom{\alpha}{m}f(t-mh)$$

- Finite Difference-Quadrature Approach:

$$F[t] = \frac{1}{\Gamma(1-\alpha)}\frac{d}{dt}\int_0^t \frac{f(s)}{(t-s)^{\alpha}}\,ds \rightarrow D^{\alpha}[f(t)] = \frac{d}{dt}F[t] \approx \frac{F(t_{j+1}) - F(t_j)}{t_{j+1} - t_j}$$

# Fractional Derivative: Numerical Approach

- Function: $f(t) = \exp(2t)$

$$F(t_{j+1}) = \chi \int_{t_0}^{t_{j+1}} \frac{f(s)}{(t_{j+1}-s)^{\alpha}} ds$$

- Area under the curve

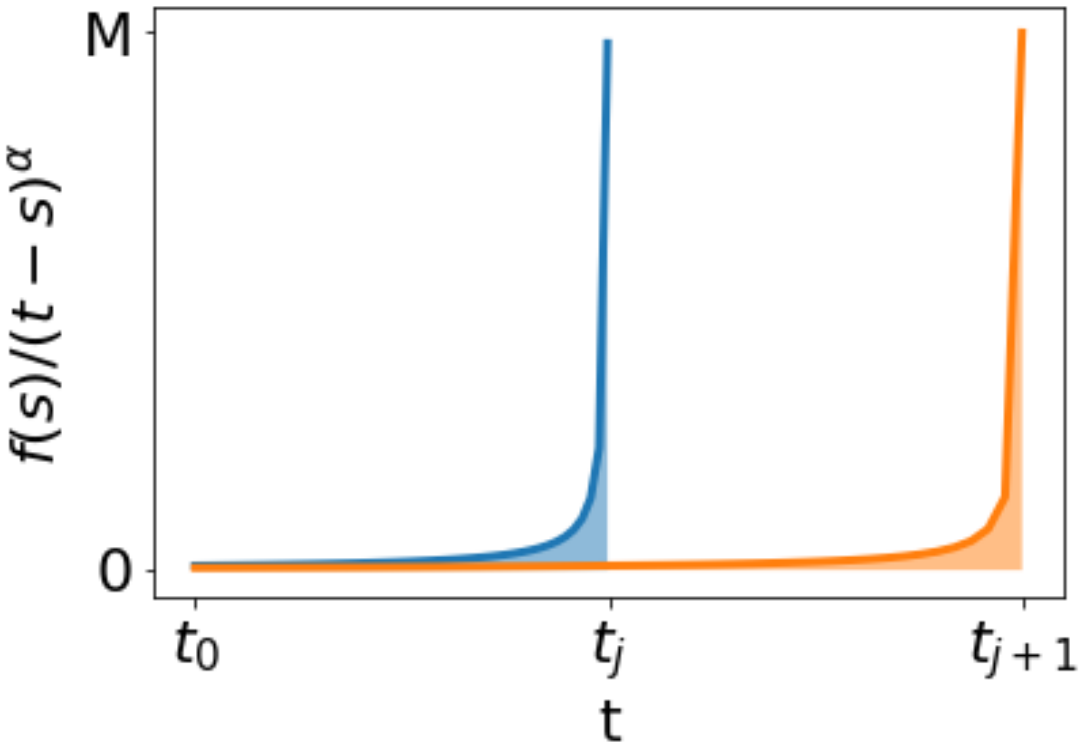


$$D^{\alpha}[f(t)] = \frac{d}{dt} F[t] \approx \frac{F(t_{j+1}) - F(t_j)}{t_{j+1} - t_j}$$

# Quadrature Methods

$$\chi = \frac{1}{\Gamma(1-\alpha)}$$

- Riemann-Sum (RS):

$$F(t_{j+1}) = \chi \int_{t_0}^{t_{j+1}} \frac{f(s)}{(t_{j+1}-s)^{\alpha}} ds \approx \chi \sum_{k=0}^{j} \frac{f(t_{k+1})+f(t_k)}{2} \int_{t_k}^{t_{k+1}} (t_{j+1}-s)^{-\alpha} ds$$

- Gaussian Quadrature (GQ):

$$F(t_{j+1}) = \chi \int_{t_0}^{t_{j+1}} \frac{f(s)}{(t_{j+1}-s)^{\alpha}} ds = \chi \sum_{i=1}^{N_q} (t_{j+1}-t_i)^{-\alpha} f(t_i) w_i$$

- Gauss-Laguerre Quadrature (GLQ): Requires extended precision!

$$F(t_{j+1}) = \underbrace{\chi \int_{t_0}^{t_{j+1}} \frac{f(s)}{(t_{j+1}-s)^{\alpha}} ds = \chi (t_{j+1}-t_0)^{1-\alpha} \int_0^1 \frac{f\left((t_{j+1}-t_0)s+t_0\right)}{(1-s)^{\alpha}} ds}_{\text{Substitute } s=\frac{t-t_0}{t_{j+1}-t_0};\ dt=(t_{j+1}-t_0)ds;\ s(t=t_0)=0,\ s(t=t_{j+1})=1}$$

# Convergence Analysis

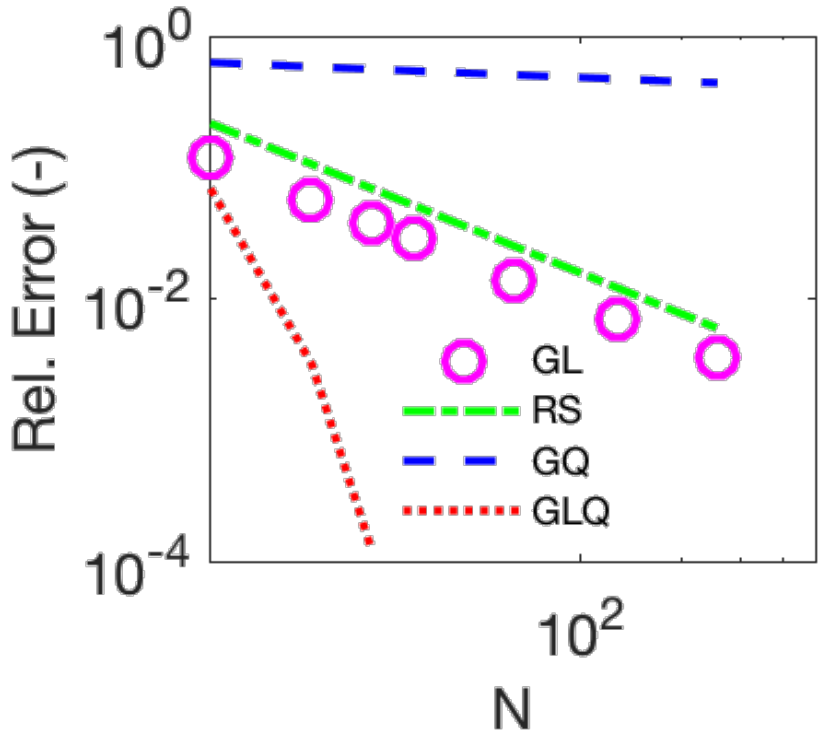


Figure: Convergence analysis using different quadrature methods for the Riemann-Liouville fractional derivative with $\alpha = 0.9$ for the test function: $f(t) = \exp(2t)$.

Table: Convergence analysis using different quadrature methods for the Riemann-Liouville fractional derivative with $\alpha = 0.9$.

| Method | $D_{RL}^{0.9}[f(t) = \exp(2t)] = 13.815$ | | | |
|---|---|---|---|---|
| | $N = 8$ | $N = 16$ | $N = 24$ | $N = 32$ |
| Grünwald-Letnikov (GL) | 12.185 | 13.019 | 13.289 | 13.422 |
| Riemann-Sum (RS) | 10.796 | 12.342 | 12.849 | 13.099 |
| Gaussian Quadrature (GQ) | 5.028 | 5.673 | 6.014 | 6.244 |
| Gauss-Laguerre Quadrature (GLQ) | 12.856 | 13.771 | 13.816 | - |

# Hyperelastic Stress

- Hybrid approach:
  - Optimal quadrature far from singularity
  - Special quadrature near singularity

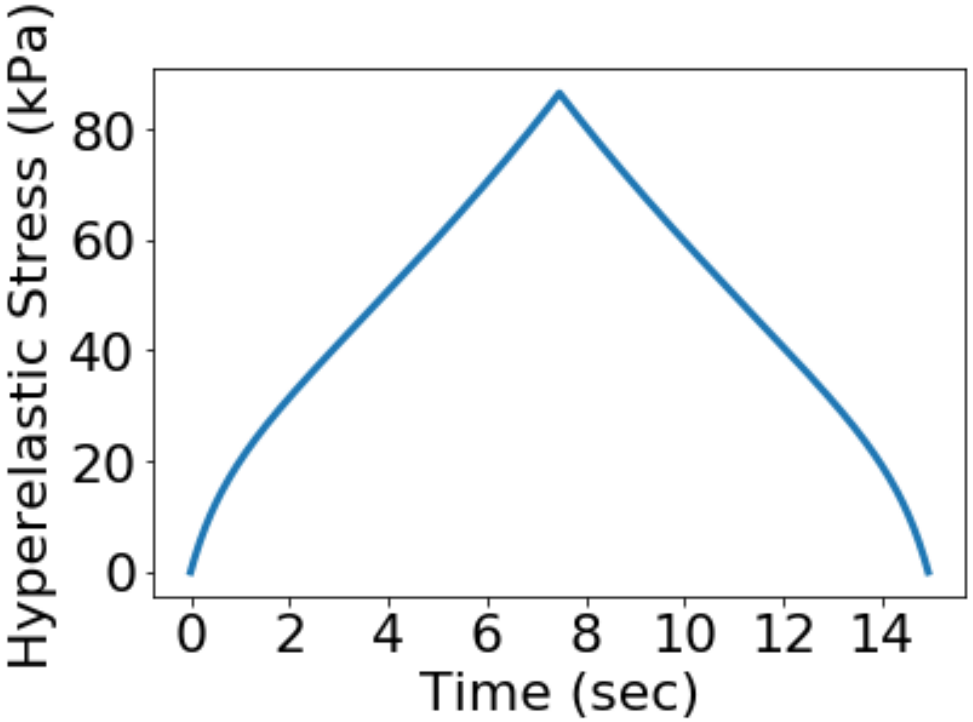


$$\int_{t_0}^{t} \frac{f(s)}{(t-s)^{\alpha}}\,ds = \underbrace{\int_{t_0}^{t-b_T} \frac{f(s)}{(t-s)^{\alpha}}\,ds}_{GQ} + \underbrace{\int_{t-b_T}^{t} \frac{f(s)}{(t-s)^{\alpha}}\,ds}_{RS}$$

# Analysis of Hybrid Methods

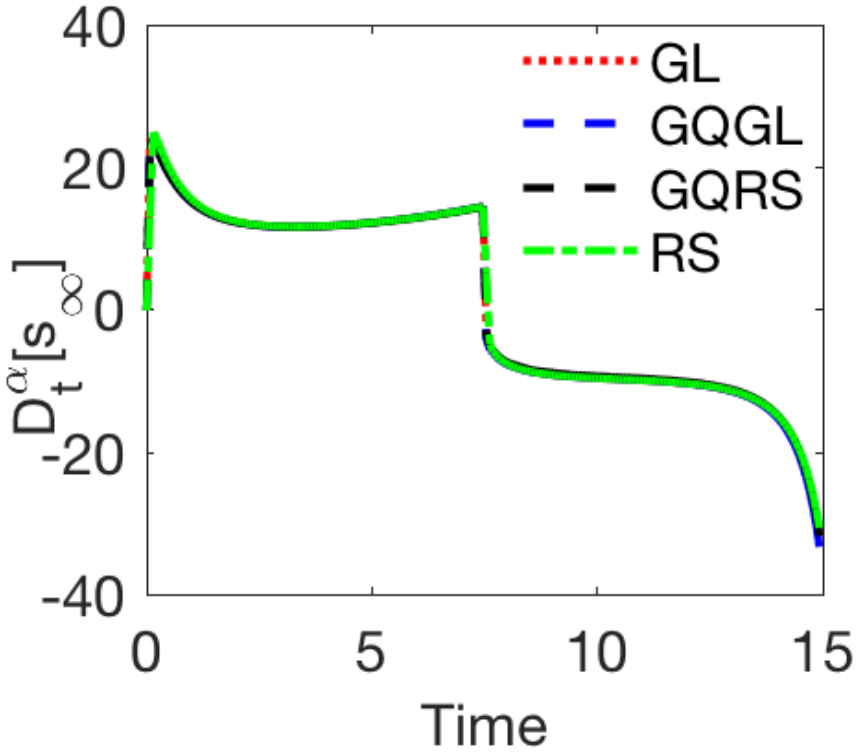


Figure: Fractional derivative of hyperelastic stress.

Table: Analysis of hybrid quadrature methods for the Riemann-Liouville fractional derivative of hyperelastic stress with $\alpha = 0.9$.

| Method | $D_{RL}^{0.9}[s_{\infty}]$ | |
|---|---|---|
| | Rel. Error | CPU-Time (sec) |
| Grünwald-Letnikov (GL) | - | 1.19 |
| Riemann-Sum (RS) | 1.88e-1 | 1.13 |
| Gaussian, Riemann-Sum Quadrature (GQRS) | 2.05e-1 | 0.27 |
| Gaussian, Gauss-Laguerre Quadrature (GQGL) | 1.09e-1 | 1.63 |

# Conclusions & Future Work:

- Tested various numerical procedures for approximating fractional derivatives.
- Gaussian Quadrature, Riemann-Sum (GQRS) maintained accuracy with significant computational improvements.
- Sensitivity analysis: hyperelastic and viscoelastic parameters
- Quantify uncertainty in sensitive parameters using experimental data.
- Explore material dependence for fractional order.

# Acknowledgements


- P.M. and W.O. thank the support provided by NSF CDS&E awards (CMMI grants 1306320 and 1306290).
- P.M., G.P., and R.S. thank the support provided by AFOSR FA9550-15-1-0299.
- Additionally, we thank Dr. M. Yousuff Hussaini and Dr. Somayeh Mashayekhi for their assistance in developing fractional order models.